

# NUMERICAL STUDY OF TURBULENT BUOYANT HELIUM PLUME BY MEANS OF ALGEBRAIC REYNOLDS STRESS AND TURBULENT SCALAR FLUX MODELS

Hitoshi Sugiyama<sup>1\*</sup>, Naoto Kato<sup>1</sup>, Masahiro Ouchi<sup>2</sup>,  
Saori Mogami<sup>3</sup>, Atsuhiko Terada<sup>4</sup>, Ryutaro Hino<sup>4</sup>

<sup>1</sup>Utsunomiya University, Graduate School of Engineering, Japan

<sup>2</sup>Shimizu Corporation, Japan

<sup>3</sup>Fuji Electric FA Components & Systems Co., Ltd., Japan

<sup>4</sup>Japan Atomic Energy Agency, Japan

## ABSTRACT

Numerical analysis has been performed for vertical buoyant turbulent flow of an air-helium mixture plume in open space by using an algebraic Reynolds stress and an algebraic turbulent scalar flux models. The results are compared with the experimental data of the velocity profile, helium concentration and Reynolds stresses to validate the presented anisotropic turbulent model. Although the agreement is certainly not perfect, especially for streamwise normal stress, the main features, which are accelerated flow, rapid diffusion of helium and periodic puff cycles induced by Rayleigh-Taylor instability, are quantitatively predicted by the presented anisotropic buoyant turbulent model. As for the discrepancy of streamwise normal stress, the cause of discrepancy is examined by using Boussinesq's eddy viscosity concept which is the basic Reynolds stress model. As a result of this examination, it was found that streamwise normal stress is decreased along the flow direction by accelerated flow. Calculated result is consistent with such characteristic feature. However, streamwise normal stress of the experiment is not satisfied with its characteristic feature. Judging from the comparison with the experiment and the examination of cause of discrepancy, the characteristic phenomena of the helium diffusion could be predicted using the algebraic Reynolds stress and turbulent scalar flux models presented in this study.

**KEYWORDS:** Turbulent flow, Helium plume, Buoyant force, Algebraic Reynolds stress model, Algebraic turbulent scalar flux model

## 1. INTRODUCTION

Buoyancy is broadly divided into buoyancy due to differences in density due to temperature changes and buoyancy caused by differences in density between matter and the surrounding matter in an isothermal field. Numerous studies have been reported with regard to buoyancy [1]. In particular, we examine the high buoyancy flow field when a gas with an extremely low density such as hydrogen or helium diffuses in air.

When the helium is discharged at relatively high speed, it moves due to convection, and appearance of a significant buoyancy effect is limited to the region quite far downstream from the jet outlet. However, when the jet outlet speed is extremely low, the propulsion force of the flow is dominated by the buoyancy arising from the difference in density between the helium and the surrounding fluid. In other words, these can be categorized into helium jet flows dominated by convection and helium plumes dominated by buoyancy due to density differences. In order to suppress convection effects as much as possible to investigate the latter case, it is necessary to measure the diffusion of the plume emitted at low speed from a jet flow.

In the case of a helium plume dominated by buoyancy due to density differences, the speed from the jet outlet is low, and a large scale is needed in order to form a turbulence field. From this perspective, O'Hern et al. [2] emitted helium from a jet outlet with a circular cross-section with a diameter of 1 m and reported the results of measuring the velocity distribution, helium concentration, and Reynolds stress in the turbulence

\*Corresponding Author: sugiyama@cc.utsunomiya-u.ac.jp

Copyright © 2019 by The Author(s). Distributed by JSME, KSME, and ASTFE with permission.

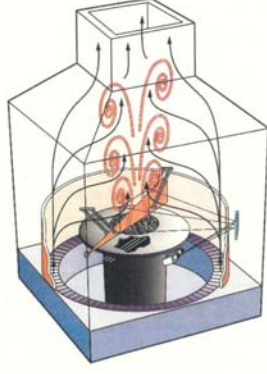


**Fig.1** Schematic diagram of experimental apparatus

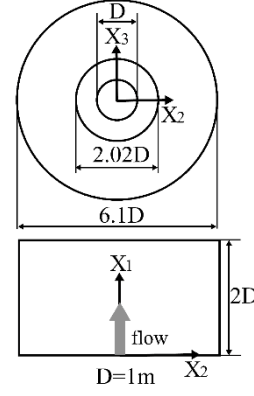


**Fig.2** Calculated domain and coordinate system

field of a helium plume dominated by buoyancy due to density differences. In the experiments, they used particle image velocimetry (PIV) to measure velocities and planar laser-induced fluorescence (PLIF) to measure helium concentration, and reported that generation of an accelerated flow, rapid diffusion of the helium concentration, and periodic variations in the streamwise velocity due to Rayleigh-Taylor instability were characteristic phenomena.

The aim of this research is to analyse the experiments of O'Hern et al. by using algebraic Reynolds stress model and turbulent scalar flux model. The pressure-scalar gradient correlation term was modeled based on a previously reported pressure-temperature gradient correlation term [3] and the model constants were selected using trial and error calculations based on consistency with the O'Hern et al. experiments. The analytical results are compared to the measured values to clarify the validity of the model.

## 2. ANALYSIS METHOD

### 2.1 Experiments Covered by Calculations

Figure 1 shows a diagram of the experimental apparatus [2] of O'Hern et al. that was used in the analysis. A disk of diameter 2.02 m was fitted around the discharge outlet from which the helium was discharged at a velocity of  $U_r = 0.325$  m/s from a circular cross-section of diameter  $D = 1$  m. The experimental apparatus fits into a cuboid space with a 6.1 m square cross-section and height of 7.3 m, and a chimney is fitted on top of that. Figure 2 shows calculation domain which is located to near the discharge outlet of helium.

### 2.2 Governing Equations

The following are the transport equations of momentum and scalar rewritten by dimensionless numbers.

$$\frac{\partial U_i}{\partial t} + \frac{\partial(U_i U_k)}{\partial X_k} = -\frac{1}{\rho} \left( \frac{\partial P}{\partial X_i} \right) + \frac{\partial}{\partial X_k} \left( \frac{1}{Re} \frac{\partial U_i}{\partial X_k} - \overline{u_i u_k} \right) + \frac{C}{Fr} \quad (1)$$

$$\frac{\partial C}{\partial t} + \frac{\partial(U_k C)}{\partial X_k} = \frac{\partial}{\partial X_k} \left( \frac{1}{Re Sc} \frac{\partial C}{\partial X_k} - \overline{u_k c} \right) \quad (2)$$

where  $U_i$  is the mean velocity in the  $X_i$  axis direction,  $C$  is the helium concentration,  $\overline{u_i u_j}$  is the Reynolds stress,  $\overline{u_k c}$  is the turbulent scalar flux,  $P$  is the mean pressure, and  $\rho$  is the density. The dimensionless numbers are the Reynolds number  $Re = U_r D / \nu$ , Froude number  $Fr = U_r^2 / gD$ , and Schmidt number  $Sc = \nu / D_i$ , where  $\nu$  the coefficient of dynamic viscosity of air is and  $D_i$  is the diffusion coefficient.

The transport equations for the Reynolds stress and turbulent scalar flux with buoyancy are shown below. In the equations,  $p$  is the pressure variation and  $\lambda$  is the scalar diffusion coefficient.

$$\begin{aligned} \frac{D \overline{u_i u_j}}{Dt} = & - \left( \overline{u_i u_k} \frac{\partial U_j}{\partial X_k} + \overline{u_j u_k} \frac{\partial U_i}{\partial X_k} \right) + \frac{p}{\rho} \left( \frac{\partial u_i}{\partial X_j} + \frac{\partial u_j}{\partial X_i} \right) - \left( g_i \overline{u_j c} + g_j \overline{u_i c} \right) \\ & - \frac{\partial}{\partial X_k} \left\{ \overline{u_i u_j u_k} - \nu \frac{\partial \overline{u_i u_j}}{\partial X_k} + \frac{p}{\rho} (\delta_{jk} u_i + \delta_{ik} u_j) \right\} - 2\nu \frac{\partial u_i}{\partial X_k} \frac{\partial u_j}{\partial X_k} \end{aligned} \quad (3)$$

**Table 1** Modeling of the pressure-strain correlation term

$\pi_{ij,1} + \pi_{ji,1}$	$-C_1 \frac{\varepsilon}{k} \left( \overline{u_i u_j} - \frac{2}{3} k \delta_{ij} \right)$
$\pi_{ij,2} + \pi_{ji,2}$	$-\frac{C_2 + 8}{11} \left( P_{ij} - \frac{2}{3} P_k \delta_{ij} \right) + \zeta k \left( \frac{\partial U_i}{\partial X_j} + \frac{\partial U_j}{\partial X_i} \right)$ $-\frac{8C_2 - 2}{11} \left( D_{ij} - \frac{2}{3} P_k \delta_{ij} \right)$
$\pi_{ij,3} + \pi_{ji,3}$	$-C_3 \left( P_{ij,c} - \frac{2}{3} P_c \delta_{ij} \right)$
$\pi_{ij,w} + \pi_{ji,w}$	$C_1 = C_1^* + C_1' f(L/X_w) \quad C_2 = C_2^* + C_2' f(L/X_w)$ $\zeta = \zeta^* + \zeta' f(L/X_w)$
$P_{ij} = -\overline{u_i u_k} \frac{\partial U_j}{\partial X_k} - \overline{u_j u_k} \frac{\partial U_i}{\partial X_k}, \quad D_{ij} = -\overline{u_i u_k} \frac{\partial U_k}{\partial X_i} - \overline{u_j u_k} \frac{\partial U_k}{\partial X_j}$ $P_k = -\overline{u_k u_i} \frac{\partial U_k}{\partial X_i}, \quad P_{ij,c} = -\left( g_i \overline{u_j c} + g_j \overline{u_i c} \right), \quad P_c = -g_i \overline{u_i c}$ $f(L/X_w) = C_\mu^{3/4} k^{3/2} / \kappa \varepsilon X_w$	

**Table 2** Model constants of the pressure-strain correlation term

$C_1^*$	$C_2^*$	$\zeta^*$	$C_1'$	$C_2'$	$C_3$	$\zeta'$	$C_\mu$	$\kappa$
1.4	0.44	-0.16	-0.35	0.12	1.8	-0.1	0.09	0.42

$$\frac{Du_i c}{Dt} = -\left( \overline{u_i u_k} \frac{\partial c}{\partial X_k} + \overline{u_k c} \frac{\partial U_i}{\partial X_k} \right) + \frac{p}{\rho} \frac{\partial c}{\partial X_i} + g_i \overline{c^2} \quad (4)$$

$$-\frac{\partial}{\partial X_k} \left\{ \overline{u_i u_k c} + \frac{pc}{\rho} \delta_{ik} - \nu c \frac{\partial u_i}{\partial X_k} - \lambda u_i \frac{\partial c}{\partial X_k} \right\} - (\nu + \lambda) \frac{\partial c}{\partial X_k} \frac{\partial u_i}{\partial X_k}$$

The Rodi approximation [4] was used for the convection and diffusion terms in each of the transport equations with the aim of increasing the computational efficiency by changing from differential to algebraic equations. The problems are the pressure-strain correlation and the pressure-scalar gradient correlation terms, which are the second terms on the right-hand sides in the Reynolds stress and turbulent scalar flux equations.

### 2.3 Modeling of the Pressure-Strain and Pressure-Scalar Gradient Correlation Terms

Tables 1 and 2 show the model equation for the pressure-strain correlation term and the constants for that model, and Tables 3 and 4 show the model equation for the pressure-scalar gradient correlation term and the constants for that model. Table 3 shows the model equation for the  $\overline{c^2}$  component of the scalar variation, which was deduced by assuming a local equilibrium state in the transport equations for the  $\overline{c^2}$  component of the scalar variation. For the model constants  $C_3$  and  $C_{3c}$  related to buoyancy, trial and error calculations were performed, and 1.8 and 1.0 were chosen for consistency with the experiments of O'Hern et al.

### 2.4 Numerical Analysis

Computational grids were placed into 68 grids along  $X_1$  and the  $X_2$  axis and  $X_3$  axis were divided into 121 grids each, for a total of 995,588 grid points. O'Hern et al. reported that the discharge velocity of the helium was 0.325 m/s. According to their velocity isoline distribution, the position corresponding to 0.325 m/s was around 0.015 m from the discharge outlet, and they measured the 0.2 m/s isoline at around 0.01 m. Since buoyancy is related to definition of  $Fr$  and important parameter. From this perspective, in this analysis, the discharge outlet velocity was set to what is thought to be a more realistic  $U_r = 0.1$  m/s, and the discharge conditions were set to the state of uniformly discharging helium of concentration 100%. This gives  $Fr = 0.102 \times 10^{-2}$  and  $Re = 6.58 \times 10^3$ . The  $Sc$  value was set to 0.21.

## 3. RESULTS AND DISCUSSION

Since the experimental results are provided with dimensions, both results were made dimensionless for comparison by using a discharge outlet velocity of  $U_r = 0.1$  m/s.

**Table 3** Modeling of the pressure-scalar gradient correlation term

$\pi_{ic,1}$	$-C_{1c} \frac{\varepsilon}{k} \overline{u_i c} - C'_{1c} \frac{\varepsilon}{k} \left( \frac{\overline{u_i u_j}}{k} - \frac{2}{3} \delta_{ij} \right) \overline{u_j c}$
$\pi_{ic,2}$	$C_{2c} \overline{u_m c} \frac{\partial U_i}{\partial X_m} - C'_{2c} \overline{u_m c} \frac{\partial U_m}{\partial X_i}$
$\pi_{ic,3}$	$-C_{3c} g_i \overline{c^2}$
$\pi_{ic,w}$	$C_{1c} = C_{1c}^* \{1 + C_{1c,w} \cdot f(L/X_w)\}$ $C'_{1c} = C'_{1c}^* \{1 + C_{1c,w} \cdot f(L/X_w)\}$ $C_{2c} = C_{2c}^* \{1 + C_{2c,w} \cdot f(L/X_w)\}$ $C'_{2c} = C'_{2c}^* \{1 + C_{2c,w} \cdot f(L/X_w)\}$
$\overline{c^2} = -\frac{1}{C_{4c}} \frac{\varepsilon}{k} \overline{u_k c} \frac{\partial C}{\partial X_k}$ $f(L/X_w) = C_\mu^{3/4} k^{3/2} / \kappa \varepsilon X_w$	

**Table 4** Model constants of the pressure-scalar gradient correlation term

$C_{1c}^*$	$C'_{1c}^*$	$C_{2c}^*$	$C'_{2c}^*$	$C_{3c}$	$C_{4c}$	$C_{1c,w}$	$C_{2c,w}$
3.9	-2.5	0.8	0.2	1.0	0.62	0.25	-0.46

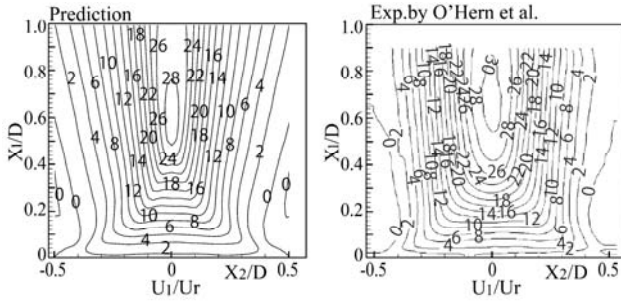


**Fig.3** Comparison of streamwise velocity

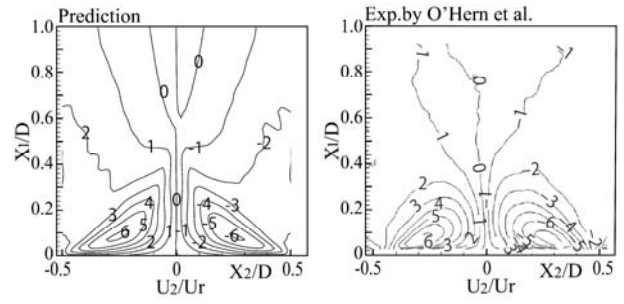


**Fig.4** Comparison of horizontal velocity

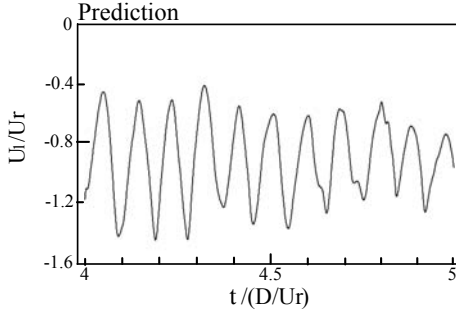


**Fig.5** Time history of streamwise velocity

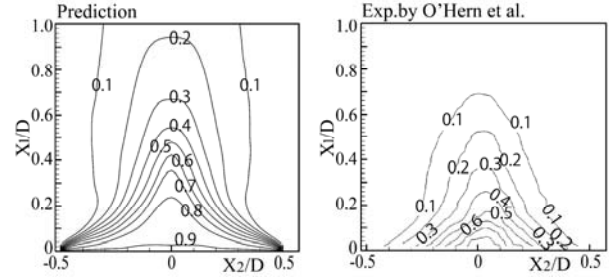


**Fig.6** Comparison of helium concentration

### 3.1 Comparison of Mean Velocity Distributions

Figures 3 and 4 show a comparison of the streamwise and horizontal mean velocity, respectively. From the compared results, it is found that the calculation predict well the measured mean velocity. Figure 5 presents the analytical results showing the time variation in the streamwise velocity at the same position as the experiments. This periodic velocity variation was reported to arise from Rayleigh-Taylor instability theory where high-density fluid descends and low-density fluid rises. Although this gives 1.78 Hz when calculated based on this periodic variation value, which is slightly different from the measured value 1.34Hz, it does reproduce the periodic velocity variation phenomenon. Figure 6 shows a comparison of the helium concentration between the two sets of results. Although the numerical analysis predicted larger values than the experimental values, it reproduced the rapid diffusion of helium.

### 3.2 Comparison of Reynolds Stress Distributions

Figure 7 shows a comparison of the turbulent energy distribution. Figures 8, 9, 10 show comparisons of the streamwise normal stress, the horizontal normal stress and shear stress, respectively. Judging from compared results, it was found that there is a significant difference from the experiments in the distribution of streamwise normal stress  $\overline{u_1^2}$ . As for the discrepancy of streamwise normal stress between calculated and measured results, the cause of discrepancy is examined by using Boussinq's eddy viscosity concept which is the basic Reynolds stress model and assumes that the turbulent stresses are proportional to the mean-velocity gradient. Boussinq's eddy viscosity concept is expressed as following equation.

$$\overline{-u_i u_j} = \nu_t \left( \frac{\partial U_i}{\partial X_j} + \frac{\partial U_j}{\partial X_i} \right) - \frac{2}{3} k \delta_{ij} \quad (5)$$

where  $\nu_t$  is turbulent eddy viscosity. Considering the definition of turbulent energy  $k$  and axisymmetric jet flow, the above equation is rewritten as following equation.

$$\overline{u_1^2} = \overline{u_2^2} - 3\nu_t \left( \frac{\partial U_1}{\partial X_1} \right) \quad (6)$$

Rewritten equation shows that streamwise normal stress is decreased and the value of streamwise normal stress is smaller than that of horizontal normal stress in accelerated flow region. This characteristic feature is consistent with the calculated result, but the experiment is not satisfied with this feature. The decrease of streamwise normal stress in accelerated flow has been measured in turbulent flow for converging hannels[5].

Besides, horizontal normal stress is also derived from Boussinq's eddy viscosity concept as following equation.

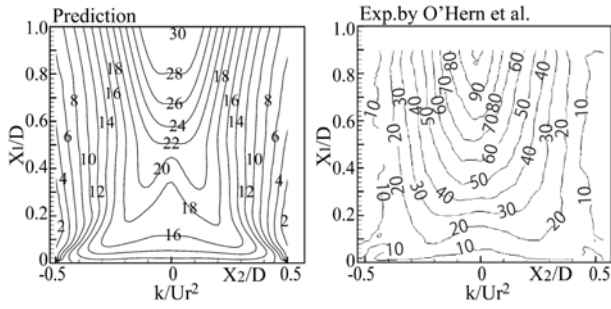


**Fig.7** Comparison of turbulent energy

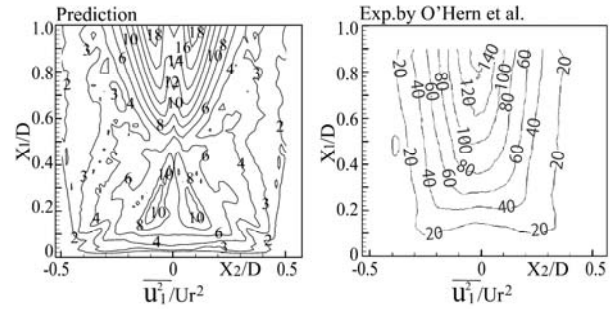


**Fig.8** Comparison of streamwise normal stress

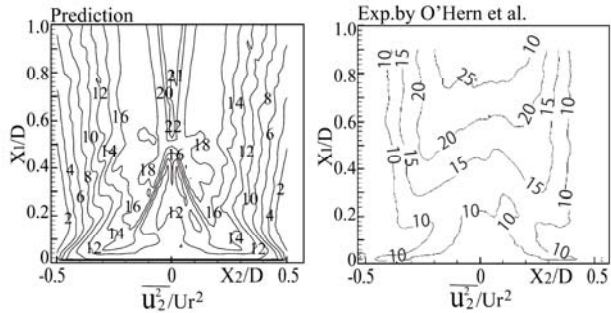


**Fig.9** Comparison of horizontal normal stress

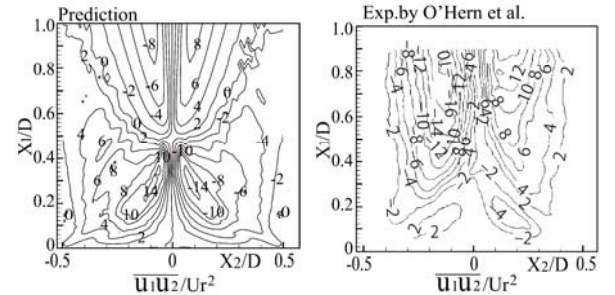


**Fig.10** Comparison of shear stress

$$\overline{u_2^2} = \frac{2}{3}k - 2\nu_t \left( \frac{\partial U_2}{\partial X_2} \right) \quad (7)$$

In the above equation, assuming that gradient of horizontal velocity is very small, the value of horizontal normal stress nearly equals to  $2k/3$ . This region is located in downward flow of helium plume as shown in horizontal velocity contour map of figure 4. The calculated result is satisfied with this relationship, while the experimental result is not consistent with this relationship.

## 4. CONCLUSIONS

Numerical analysis has been performed for vertical buoyant turbulent flow of helium plume. Although the agreement is certainly not perfect, especially for streamwise normal stress, the main features, which are accelerated flow, rapid diffusion of helium and periodic puff cycles induced by Rayleigh-Taylor instability, are quantitatively predicted. Judging from the comparison with the experiment and the examination of cause of discrepancy, the characteristic phenomena of the helium diffusion could be predicted using the algebraic Reynolds stress and turbulent scalar flux models presented in this study.

## ACKNOWLEDGMENTS

The present study was performed in the Advanced Nuclear Hydrogen Safety Research Program entrusted by Agency for Natural Resources and Energy of Ministry of Economy, Trade and Industry. We deeply express special thanks for supporting research work.

## REFERENCES

- [1] Panchapakesan, N.R., and Lumley, J.L., "Turbulence measurements in axisymmetric jets of air and helium. Part 2. Helium jet," *J. Fluid Mech.*, Vol.246, pp.225-247 (1993).
- [2] O'Hern, T.J., Weckman, E.J., Gerhart, A.L., Tieszen, S.R., and Schefer, R.W., "Experimental study of a turbulent buoyant helium plume," *J. Fluid Mech.*, Vol.544, pp.143-171 (2005).
- [3] Sugiyama, H., Akiyama, M., Nemoto, Y., and Gessner, F.B., "Calculation of turbulent heat flux distribution in a square duct with one roughened wall by means of algebraic heat flux model," *Int. J. Heat and Fluid Flow*, Vol.23, pp.13-21 (2002).
- [4] Rodi, W., "A new algebraic relation for calculation the Reynolds stresses," *Z. Angew. Math. Mech.*, Vol.56, pp.219-221 (1976).
- [5] Shah, M.K., and Tachie, M.F., "PIV study of turbulent flow in asymmetric converging and diverging channels," *Transactions of ASME, Journal of Fluids Engineering*, DOI: 10.1115/1.2829590.